Generator Out-of-Step Protection Using the Trajectory of Estimated Relative Speed

Kasun Samarawickrama, Athula D. Rajapakse, Nuwan Perera

***Abstract*—The condition where the load angle of a generator changes rapidly with respect to another generator or portion of a system is called Generator Out-of-Step (OOS). The traditional way of detecting an OOS condition is to analyze the trajectory of the impedance seen from the generator terminals. Therefore, setting calculations for these impedance-based methods become more challenging and time consuming. Detailed time domain simulations, which required both generator and system data, are necessary to set up these relays. This paper proposes a novel method to detect an OOS condition of a generator using its relative rotor speed. The inputs for the proposed algorithm are the terminal voltage, current and machine parameters which are readily available for typical synchronous generators. The proposed algorithm monitors the change of relative rotor speed following a fault and declares the OOS condition if the relative speed tends to increase during a swing cycle. This technique is computationally simple, easy to implement, and fast compared to impedance-based methods. The application of the proposed method is investigated using time domain simulations. Also, the sensitivity and security of the proposed method are analyzed under various power system conditions.**

***Keywords*—Generator Out-of-Step, synchronous generator, speed estimation, angular instability, power swing.**

I. Introduction

POWER systems subject to a broad range of disturbances during their operation. These disturbances may cause power oscillations between individual generators, interconnected systems or both. These electromechanical oscillation may lead to voltage and/or angular instabilities which may ultimately result in loss of synchronism. Since the prime movers try to maintain a constant (synchronous) speed at their turbines, these power oscillations can cause generators to slip poles, resulting in torsional stresses in their mechanical systems. Increased rotor iron currents, winding stresses and oscillatory torques may also be observed as subsequent consequences [1]. All of these effects are potentially damaging to the generator. In order to avoid such equipment damages, prompt disconnection of the systems or generators which are operating asynchronously using Out-Of-Step (OOS) protection schemes is important [2].

At present, there are several methods to provide generator OOS protection using system and generator variables. One of the popular and heavily used OOS relays is based on the impedance measured at the generator terminals [3], [4]. Loss of Excitation (LOE), Mho, blinders, lens and concentric circles are the major types of characteristics used in impedance-based OOS schemes [2], [5]–[9]. The LOE scheme measures the impedance looking into the generator, therefore it cannot detect swings passing through the generator step-up transformer (GSU). Mho scheme is normally set to see the generator transient reactance ($X_d{}'$) plus the GSU impedance (X_t). This setting would not detect slow moving swings, where the generator synchronous reactance (X_d) would be the appropriate model. The blinder, lens and concentric circle schemes provides reliable protection but calculating settings for these schemes is more challenging and requires detailed dynamic simulations, which includes both generator and the system data [10]–[12]. As an example, the critical rotor angle is used to calculate the settings for a blinder scheme. To identify the critical rotor angle, a transient stability study which includes the modelling of generation plant dynamics and network is required. To ensure the most accurate results, the simulation must consider the most challenging condition, which provides the shortest swing time between the blinders during an out-of-step condition.

Rate of change of swing center voltage (SCV) is used to detect an OOS condition in the algorithm presented in [13]. This is a novel scheme which relies upon an assumption that the system impedance angle is close or equal to $90°$. This is the main disadvantage of this method since the impedance angle is not guaranteed to be close to $90°$ for all system conditions (e.g. for a systems with high damping ratio). References [2], [14] and [15] discuss rate of change of resistance (Rdot) and rate of change of impedance based schemes, where the terminal resistance or impedance and its rate of change is used to detect an unstable swing. These schemes cannot be set to operate for a specific angle separation.

Several equal area criteria based schemes discussed in [16]–[23] and an adaptive scheme described in [18] use voltage and current measurements from several locations of the network. These schemes use this wide area information to calculate the power angle following a system event. The main drawback of these schemes is the requirement of measuring and communication devices, such as PMUs and PDCs. In the scheme described in [19], [20], one of the parameter use to detect an unstable swing is rate of change of real power. Since this parameter is based on the maximum slip frequency, extensive time domain simulation studies are required to calculate a reasonable threshold setting.

The algorithm described in [24] uses terminal voltage acceleration and angular velocity to detect an OOS condition.

The authors are with the Department of Electrical and Computer Engineering, University of Manitoba, Winnipeg, MB R3T 5V6 (emails: samarawk@myumanitoba.ca; athula.rajapakse@umanitoba.ca; nuwan.perera@umanitoba.ca). Kasun Samarawickrama is also with Electranix Corporation Winnipeg, MB R3Y 1P6 and Nuwan Perera is also with Stantec Inc. Winnipeg, MB R3B 2B9

Paper submitted to the International Conference on Power Systems Transients (IPST2023) in Thessaloniki, Greece, June 12-15, 2023.

The scheme monitors the angular velocity and the trip signal is issued at a positive-going zero crossing of the voltage acceleration. Reference [25] discusses a technique where the deviation of speed and power are used to detect an OOS condition. The method discussed in [26] uses the state plane trajectory analysis to calculate the critical clearing time, and hence to detect an OOS condition. The scheme discussed in [21] declare an OOS condition if the integrated area under power vs time curve during the first cycle following a disturbance is less than or equal to zero. One of the major disadvantage in all the schemes discussed in [19]–[21], [24]–[26] is that the angle at which tripping is issued cannot be adjusted. This is very important when the breaker is not adequate for OOS duty. Also, these schemes cannot distinguish between a generator and line OOS condition.

A flux-based method for OOS protection of synchronous generators is described in [27]. The angular velocity and acceleration calculated from the measured magnetic flux are used to detect the OOS condition. The trip signal is issued at the point where the polarity of the angular acceleration changes from a negative to a positive value and the angular velocity is greater than the rated value. The main drawback of this method is the requirement of physical sensors to measure the stator magnetic flux. Reference [28] introduces a method that uses wavelet transform to detect power swings as well as faults during power swings. Wavelet Transform use high processing rates to capture the energy of the transients for all faults at any location, instant and prefault condition. Therefore, the major disadvantage of this scheme is high computational cost due to increased calculations per second.

In this paper, a simple new method is proposed to detect the OOS condition of a generator using the generator's relative speed vs time trajectory. The proposed algorithm monitors the trajectory of relative speed following a fault and declares the OOS condition if it follow a certain pattern. The proposed OOS detection method is validated using time domain simulations performed on a test system using the electromagnetic transient (EMT)-type simulator, PSCAD/EMTDC [29]. The sensitivity of the proposed method to various power system aspects is also analyzed.

The paper is organized as follows. In section II, the development of the proposed scheme, including both estimation of relative speed and OOS detection algorithms, has been described. Section III contains the implementation and validation of the proposed scheme using PSCAD/EMTDC. In Section IV, the results of case studies performed on a five bus system are presented. Finally, concluding remarks are presented in Section V of this paper.

II. Proposed Out-of-Step Protection Scheme

The proposed method is developed based on the generator's relative speed of rotation which is a direct indicator of OOS condition as the energy imbalance in a generator due to a disturbance causes the speed variations. The proposed method detects the OOS condition of a generator using its relative speed vs time trajectory. The relative speed is calculated using the terminal quantities (voltage and current) along with generator parameters. The proposed algorithm monitors the trajectory of relative speed following a fault and declares the OOS condition if it crosses certain thresholds. A basic connection diagram of proposed OOS relay and its main computing blocks are depicted in Fig. 1.

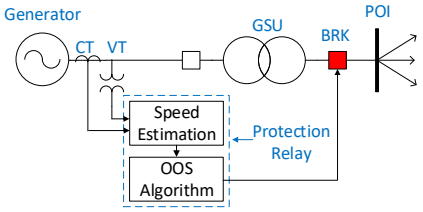

Fig. 1: Basic connection diagram of proposed OOS relay

A. Estimation of Relative Speed

The estimation of generator's relative speed using its terminal quantities and machine parameters is given below. The effect of stator transients on the calculation of relative speed is not essential for the purpose of OOS detection. Therefore, stator transients can be neglected in the calculation. Further details of stator transients are discussed in section II-C and the assumption of neglecting stator transients in the OOS detection algorithm is validated in section IV-A.

The per unit value of instantaneous electrical power output from the generator is calculated as;

$$P_t = \frac{v_a \cdot i_a + v_b \cdot i_b + v_c \cdot i_c}{S_{base}} \tag{1}$$

where;

v_a, v_b, v_c = instantaneous terminal phase to neutral voltages
i_a, i_b, i_c = instantaneous terminal currents
S_{base} = rated MVA of the generator

Per unit electrical power loss due to stator resistance is calculated as;

$$P_r = \frac{\left(I_a^2 + I_b^2 + I_c^2\right) \cdot R}{S_{base}} \tag{2}$$

Where I_a, I_b and I_c are the digital RMS quantities of i_a, i_b and i_c, respectively. R is the stator resistance and S_{base} is the rated MVA of the generator. The calculation of digital RMS (X) of an instantaneous signal $x(t)$ is given below.

$$X = \sqrt{\frac{1}{N} \cdot \sum_{n=1}^{N} \left[x(t - (N-n)\Delta t)\right]^2} \tag{3}$$

where, N = number of samples per cycle, t = present time and Δt = sample time, which is calculated as;

$$\Delta t = \frac{1}{f \cdot N} \tag{4}$$

with f being the base frequency. The converted power in the generator,

$$P_e = P_t + P_r \tag{5}$$

where; P_t = output electrical power and P_r = resistive losses in the stator. From the rule of energy conservation, the pre-fault mechanical power is calculated as, $P_m = P_e$. The calculated pre-fault mechanical power is smoothed by applying the digital

RMS calculation as in (3) to account for any harmonic power (if exist);

$$P_m = \sqrt{\frac{1}{N} \cdot \sum_{n=1}^{N} \left[P_e(t-(N-n)\Delta t)\right]^2} \tag{6}$$

Assuming the governor's response is comparatively slow, and the mechanical power is constant during the fault and immediate post fault period, the relative speed ($\Delta\omega$) is calculated using (5), (6) and the swing equation [30] as;

$$\frac{2H}{\omega_s} \cdot \frac{d^2\delta}{dt^2} = P_a = P_m - P_e \tag{7}$$

$$\Delta\omega = \frac{d\delta}{dt} = \int_{t_0}^{t} \frac{\omega_s}{2H}\left(P_m - P_e\right) dt \tag{8}$$

where;

H = inertia constant of the generator (s)
ω_s = rated speed of the generator (in per unit, $\omega_s = 1$), and
P_a = acceleration power

B. OOS Detection Algorithm

Two examples of the relative speed vs. time characteristics, one for a stable power swing and the other for an unstable power swing are shown in Fig. 2.

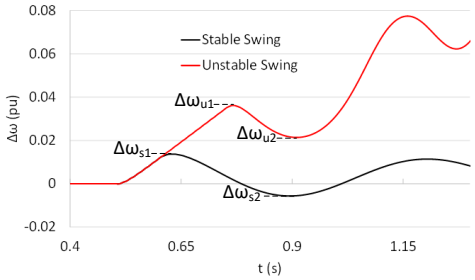

Fig. 2: Typical $\Delta\omega$ trajectories for stable and unstable power swings

At steady state, the per unit relative speed is at zero (speed is at 1 pu). During the fault, relative speed increases until the fault is cleared. In the example shown in Fig. 2, both faults are applied at 0.5s and cleared at 0.6s (6 cycles) and 0.75s (15 cycles) creating stable and unstable power swings, respectively. Once the fault is cleared, the relative speed changes based on the stability of the power swing. For a stable power swing, the relative speed oscillates around time axis and eventually settles at zero. For an unstable power swing, the relative speed keeps increasing and the poles keep slipping until the generator trips.

The above-described nature of a generator's relative speed after fault clearance is used in the proposed algorithm to detect an OOS condition. The proposed algorithm declares a power swing as an unstable swing if the relative speed measured at the fault clearance ($\Delta\omega_{u1}$) and at the first dip (or peak) ($\Delta\omega_{u2}$) have the same polarity. Similarly, a stable condition is declared if the relative speed measured at the fault clearance ($\Delta\omega_{s1}$) and at the first dip (or peak) ($\Delta\omega_{s2}$) have opposite polarities. The algorithm can be set to check the polarity of second and two consecutive dips and peaks instead of the first two if the generator allows one or several pole slips.

The dips or peaks of relative speed trajectory are identified by the zero crossings of the derivative of relative speed. The relay pickup and reset functions are based on the comparison of estimated relative speed against a user defined threshold settings. These threshold settings are not active protection settings where the timing of the trip signal is affected. They are rather a set of settings where the activation and deactivation of the relay is based on. If the estimated speed exceeds the pick up threshold value, the OOS relay picks up and starts storing the relative speeds at dips (or peaks) in an array of memory to be used by the OOS detection function.

The reset function operates when the relative speed at a dip (or a peak) is lower than the reset threshold value for a period longer than two cycles. It is highly unlikely that the power swing will be unstable once the relative speed reduced beyond the reset threshold for a period of two cycles (unless a secondary power swing occurs before the first swing is fully settled). In other words, the two-cycle setting ensures that the oscillation is well damped. The calculation of two-cycle period is based on the slip frequency which is calculated using the zero crossings of the relative speed.

A block diagram of the proposed OOS detection algorithm is depicted in Fig. 3.

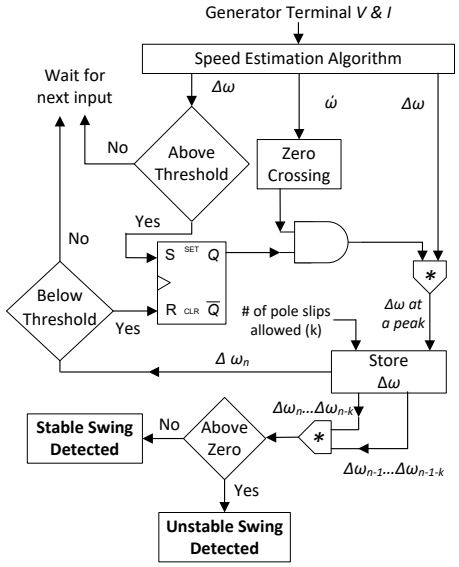

Fig. 3: Combined OOS detection algorithm

C. Effect of Stator Transients on Relative Speed

The effect of stator transients on the calculation of generator's relative speed is analyzed in this section. Equations for the synchronous generator stator circuit voltage can be written as [30], [31];

$$v_a = \frac{\mathrm{d}\psi_a}{\mathrm{dt}} - Ri_a = p\psi_a - Ri_a \tag{9a}$$

$$v_b = p\psi_b - Ri_b \tag{9b}$$

$$v_c = p\psi_c - Ri_c \tag{9c}$$

where;

v_a, v_b, v_c	= instantaneous stator induced EMF (L-G)
i_a, i_b, i_c	= instantaneous stator currents in phases a, b, c
R	= armature resistance per phase
p	= differential operator d/dt

The flux linkage in the phase a at any instant is given by

$$\psi_a = -l_{aa}i_a - l_{ab}i_b - l_{ac}i_c + l_{afd}i_{fd} + l_{akd}i_{kd} + l_{akq}i_{kq} \quad (10)$$

where;

l_{aa}, l_{bb}, l_{cc}	= self inductance of stator windings
l_{ab}, l_{bc}, l_{ca}	= mutual inductance between stator windings
l_{afd}, l_{akd}, l_{akq}	= mutual inductance between stator and rotor windings
i_{fd}, i_{kd}, i_{kq}	= field and amortisseur circuit currents

Similar expressions apply to flux linkages of windings b and c. The negative sign associated with the stator winding currents is due to their assumed direction. All the inductances in (10) are functions of the rotor position and are thus time-varying.

As explained in Section II-A, the instantaneous electrical power output from the generator is calculated as;

$$P_t = v_a \cdot i_a + v_b \cdot i_b + v_c \cdot i_c \quad (11)$$

We can eliminate phase voltages and currents in terms of the $dq0$ components using the Park's transformation [32].

Applying Park's transformation on (11) gives;

$$P_t = \frac{3}{2}(v_d \cdot i_d + v_q \cdot i_q + 2 \cdot v_0 \cdot i_0) \quad (12)$$

Equations (9a) to (9c) are basic equations for phase voltages in terms of phase flux linkages and currents. Application of the $dq0$ transformation on (9a) to (9c) gives [30];

$$v_d = p\psi_d - \psi_q p\theta - Ri_d \quad (13a)$$

$$v_q = p\psi_q + \psi_d p\theta - Ri_q \quad (13b)$$

$$v_0 = p\psi_0 - Ri_0 \quad (13c)$$

The angle θ is the angle between the axis of phase a and the d-axis. The term $p\theta$ in the above equations represents the angular velocity (ω_r) of the rotor. Substituting v_d, v_q and v_0 in (12) with (13a) to (13c) and rearranging, an expression for P_t can be obtained as;

$$\begin{aligned} P_t = \frac{3}{2}[&(i_d p\psi_d + i_q p\psi_q + 2i_0 p\psi_0) \\ &+ (\psi_d i_q - \psi_q i_d)\,\omega_r \\ &- \left(i_d^2 + i_q^2 + 2i_0^2\right) R] \end{aligned} \quad (14)$$

$$\begin{aligned} P_t = &\text{(Rate of change of armature magnetic energy)} \\ &+\text{(power transferred across the air gap)} \\ &-\text{(armature resistance loss)} \end{aligned} \quad (15)$$

Ideally, the electrical power responsible for the acceleration of the rotor is the power transferred across the air-gap. Therefore, in the exact calculation of relative speed in (8), the term P_e should be calculated using both "armature resistance loss" and "rate of change of armature magnetic energy".

The term "rate of change of armature magnetic energy" or in other words the transformer voltage term ($p\psi_d$, $p\psi_q$) represents the stator transients, which prevent ψ_d and ψ_q from changing instantaneously. It is the phenomenon that produces the dc offset in the fault currents. The omission of $p\psi_d$, $p\psi_q$ terms would therefore, eliminate the dc offset and its related effects on the dynamic performance of the generator.

The stator transients usually exist during a fault or disturbance and decay within a much shorter time compared to the time scale of rotor speed variations.Therefore, the effect of transient currents can be ignored without much error. Further, the proposed OOS detection method is not affected by neglecting stator transients because the OOS condition usually occurs when the disturbance is cleared where the stator transients are minimal.

III. Implementation in an EMT Program

A. Implementation of Proposed Method

The proposed method is implemented as a custom component in PSCAD/EMTDC Version 4.6.3. The model is built using control blocks and custom components that were written using Fortran 95 programming language and compatible for Intel Fortran version 9.0 or higher. The simulation time step is set to $10\mu s$. The actual relay calculations are performed at 64 samples per cycle (time step of $260.4167\mu s$). Since these time steps are not integer multiples, the voltage and current measurements are interpolated to obtained values of each calculation time stamp (e.g. measurements at $260\mu s$ and $270\mu s$ are interpolated to obtain the values at $260.4167\mu s$). The implementation of two algorithms are discussed below.

1) Relative Speed Estimation Algorithm: The relative speed estimation is performed in every calculation step. If the relay is not being picked up (i.e. $\Delta\omega$ is less than pickup threshold), then the mechanical power input of the generator is assumed as the power transferred across the air-gap (i.e. the summation of instantaneous electrical power and resistive losses when stator transients are neglected, see (15)). The digital RMS model in PSCAD is used to calculate resistive losses.

When expressed in p.u., acceleration torque is equal to acceleration power. Therefore, all power values are converted into per unit values on the machine base. Then the relative speed is calculated by integrating the swing equation of the machine (8) by applying trapezoidal integration. This gives,

$$\Delta\omega = \frac{\omega_s}{2H}P_m - \frac{\omega_s}{2H}\left[\left(\frac{P_e(t_1) + P_e(t_2)}{2}(t_2 - t_1)\right)\right] \quad (16)$$

where; t_2 and t_1 are time stamps of present and previous time steps, respectively.

The machine inertia constant and the stator resistance are the only input data used other than the measured voltages and currents. The rated speed is added to the output of integrator ($\Delta\omega$) to obtain the machine speed (ω) for comparison purposes.

2) OOS Detection Algorithm: The two main outputs of the speed estimation algorithm, namely, relative speed and the rate of change of speed ($\dot{\omega}$),which is linearly proportional to acceleration power are used as inputs for the OOS detection algorithm. The relay pickup and reset functions are

implemented using level comparators and a Set/Reset latch model. If relative speed is greater than the pickup threshold, then the relay picks up and latches until the reset function activates.

The pickup and reset thresholds of relative speed are set to 0.001 pu and 0.0005 pu. These thresholds are chosen such a way that the relay will not pick up for minor system oscillations and also pick up fast enough during power swings to detect the first pole slip. In other words, the final decision of the relay or the timing of the trip signal is not affected by this threshold setting (unless the threshold setting is too large and misses the first pole slip).

Once the relay is picked up, the relative speed at every positive and negative peak is stored in an array of memory until a trip or reset signal is issued. The peak/valley point of relative speed is detected by observing the zero crossing of rate of change of speed ($\dot{\omega}$) trajectory. Adjacently stored relative speeds are multiplied with each other and compared against zero using a level comparator to detect whether the speed oscillation is stable or unstable. If the adjacent speeds have the same sign, the speed is either continuously increasing or decreasing. Hence the algorithm declares an unstable power swing and issues a trip signal. The number of relative speed pairs to check can be adjusted based on number of pole slips allowed before tripping. Similarly, if the adjacent relative speeds have different signs, indicating that the speed oscillation is damping, the algorithm declares that the oscillation is stable and a trip signal will not be issued. Ultimately, when the stored relative speed is less than the reset threshold, relay rest signal is issued.

B. Implementation of Other OOS Algorithms

To compare the performance of the proposed method against existing methods, a well established traditional method and a relatively novel terminal voltage based method from literature were implemented in PSCAD/EMTDC. Double blinder method [2], [7]–[9] and the rate of change voltage (ROCOV) method [33] were selected as the candidates for comparison purposes. The ROCOV method is originally developed for transmission line OOS protection in reference [33] and the same concept is applied for generator OOS protection in this paper.

C. Implementation of Test Network

All tests were performed on the five bus example network given in the “IEEE tutorial on the protection of synchronous generators" by IEEE power system relaying committee [7]. A single line diagram of the test network is depicted in Fig. 4. The network and generator parameters can be found in [34].

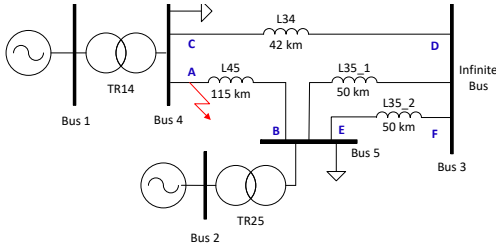

Fig. 4: The example network used for EMT simulations

IV. Results

The results of three sets of tests performed on the test network in Fig. 4 is presented in Sections IV-A through IV-C.

A. Stator Transients

Two tests were performed to validate the assumption of neglecting the effect of stator transients on the calculation of relative speed. A fault is applied on the Bus 4 end of the transmission line between Bus 4 and Bus 5 ($L45$) and the line was tripped to clear the fault. The duration of the fault was adjusted to 6 cycles and 15 cycles to create stable and unstable power swings. The calculation of stator transients was done by using (13) and (14) using the generator rotor speed and $dq0$ components of the stator fluxes, voltages and currents available via internal monitoring signals of PSCAD synchronous machine model [29].

Fig. 5 shows the calculated rotor speed by neglecting and including the stator transients for the stable and unstable power swings. The traces where the speed is calculated by including stator transients show a slight oscillation during fault, which decays after the fault is cleared. In fact the oscillation amplitude decayed during the fault itself. Since OOS condition generally occurs after the fault clearance, the effect of stator transients for the proposed technique is negligible. Moreover, inclusion or omission of stator transients does not affect the OOS trip decision. The amplitude difference between the speeds in the Fig. 5 is due to the error accumulated from the integration due to omission of stator transients.

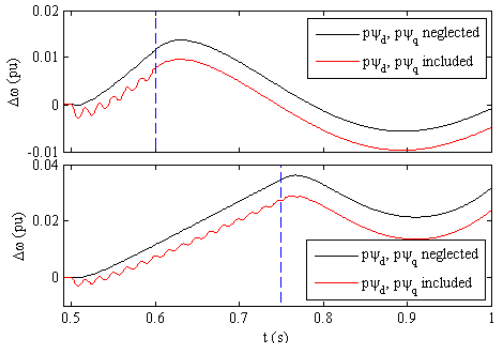

Fig. 5: Effect of neglecting stator transients on estimated relative speed (fault clearance is shown in blue dotted line)

B. Sensitivity Analysis

Sensitivity of the proposed method to different types of exciters, governors, power system stabilizers (PSS), inertia constants (H), CT and VT errors, system faults, line opening, load and generator tripping were investigated. These sensitivities are categorized under four sections as below.

- Generator configuration - 5 scenarios
- Measurement errors - 5 scenarios
- System Faults (large disturbances) - 96 scenarios
- Tripping without faults (small disturbances)- 7 scenarios

All the sensitivity tests were performed on the same five bus example network described in section III-C. All together, hundred and thirteen (113) different scenarios were analysed. Details of each category above are explained below.

1) Sensitivity for generator configuration: To analyse the sensitivity of the proposed method on the generator configuration, a number of standard exciters, governors and PSSs were used with the proposed relay model in EMT simulations. For the sensitivity tests of inertia constant a $\pm 10\%$ and $\pm 20\%$ errors were introduced to the generator's inertia.

Results showed that the effect from exciter, governor and PSSs was minimal during the focused period due to large mechanical and electrical time constants involved. Therefore, significant differences were not observed in the calculated speed and the comparison plots were omitted. The results of inertia constant tests are depicted in Fig. 6. Under different inertia constants, the estimated speed is deviating from its actual value. However the timestamps of the peaks and dips are more or less aligned with each other. Therefore, the trip decisions are made at around the same time in all cases regardless of the magnitude of the error introduced. It is possible that the relay can mis-operate if the magnitude of error makes the calculated relative speed stop crossing the x-axis during the first dip. The magnitude of error required for a mis-operation is based on how stable the power swing is and whether the relay allowed a single pole slip.

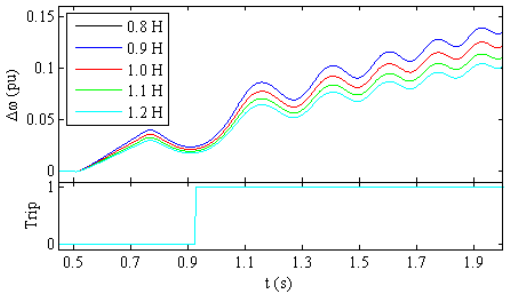

Fig. 6: Sensitivity of the relative speed to inertia constant

2) Sensitivity for measurement errors: To mimic the errors of measurement devices, a $\pm 10\%$ and $\pm 20\%$ errors were introduced to measured terminal voltages and currents.

The results are depicted in Fig. 7. Similar to inertia constant tests results, the estimated speed is deviating from its actual and the timestamps of the peaks and dips are more or less aligned with each other. Therefore, the trip decisions are made at around the same time in all cases regardless of the magnitude of the error introduced.

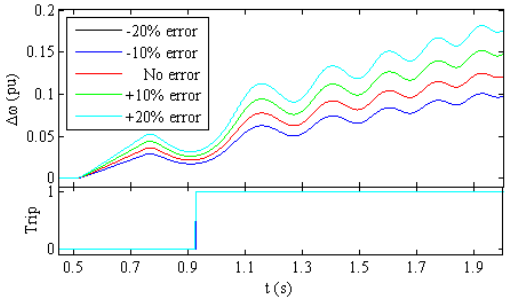

Fig. 7: Sensitivity of the relative speed to measurement errors

3) Sensitivity for system faults: Ninety six (96) unique fault scenarios were simulated to test the sensitivity and security of the proposed method. This includes, four fault types (LG, LLG, LLLG and LL), six fault locations (A-F in Fig. 4), two fault durations (200 ms and 600 ms) and two fault impedances (0.001 and 5 ohms).

Summary of the test results is tabulated in I. As shown below, the majority of simulated scenarios created stable power swings (81 out of 96) and as expected, relay did not pick up for any of those stable swings. Fifteen (15) scenarios out of ninety six (96) observed to have unstable power swings. The proposed algorithm issued the trip signal at the first pole slip in all unstable scenarios except for one. It missed the first pole slip in one scenario due to marginal errors in the speed estimation algorithm. However, OOS detection algorithm issued the trip signal at the second pole slip (see Fig. 8). Overall, the proposed algorithm has shown success rate of 98.96% for system faults.

TABLE I: Statistical results summary of system fault events

Description	**Number of Scenarios**		
	Simulated	**Detected Correctly**	**Mis/Mal Operated**
Unstable Power Swings	15	14	1
Stable Power Swings	81	81	0
Total	96	93	3
Total as %	100 %	98.96 %	1.04 %

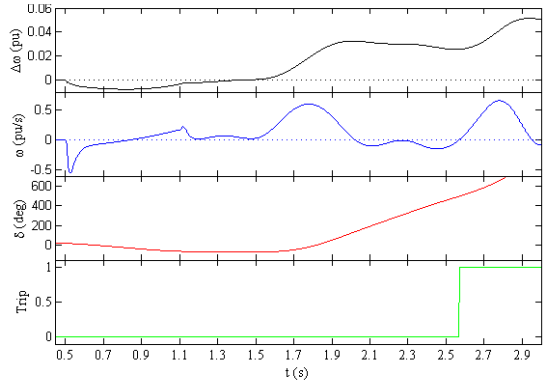

Fig. 8: Marginal mis-operation of the proposed algorithm at the first pole slip and correct operation at the second slip

4) Sensitivity for small disturbances: Seven (7) unit tripping scenarios with no faults were analysed under this category. This includes four transmission line openings ($L34$, $L45$, $L35\_1$ and $L35\_1 + L35\_2$), two load disconnections (at bus 4 and 5) and one generator disconnection (for this disturbance, the test system is slightly modified by duplicating the generator at bus 2 for the purpose of tripping one). Five out of seven scenarios created stable power swings in the test network. Unstable power swings were created in the bus 4 load tripping scenario and the bus 2 generator tripping scenario. In all seven scenarios, the relay successfully detected stable or unstable power swings. Fig. 9 shows the results of generator tripping scenario where OOS condition is occurred due to deceleration of the machine.

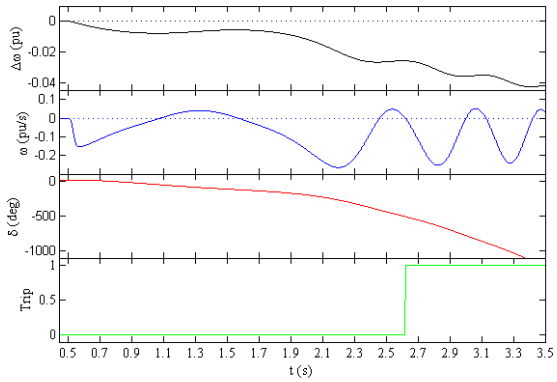

Fig. 9: Generator OOS condition due to deceleration

C. Comparison with Other Methods

OOS detection speed and security of the proposed method was compared against double blinder and rate of change voltage (ROCOV) schemes [33]. Both methods were implemented in PSCAD/EMTDC as described in section III-B. The same two faults as in section IV-A were applied on the test network to create stable and unstable power swings. The comparisons of results are illustrated in Figs. 10 to 14.

As shown in Fig. 14, the ROCOV scheme delivered the fastest tripping for an unstable power swing. Unlike impedance base methods or the proposed method (where the trip decision is made using two measured quantities), the ROCOV trip decision is made based on a single measured quantity crossing of a user-defined boundary. Therefore, ROCOV characteristic can be highly influenced by the dynamics of rest of the system. Hence it is difficult to calculate a single ROCOV settings which works for all the conditions. In other words, generalization the operation of ROCOV scheme is strenuous. The settings used for this example is obtained by several time domain simulation iterations ranging from stable power swings to highly unstable power swings for many network conditions. Fig. 11 shows the user-define boundary and the ROCOV vs DV trajectories.

Compared to the double blinder scheme, the proposed method has operated faster (see Fig. 14). This is because the proposed method has issued the trip signal at the first pole slip while the double blinder scheme has issued the trip signal when the calculated impedance is leaving the supervisory Mho circle following the first pole slip (i.e. trip on the way out). When the blinder scheme is set to “trip on the way in”, faster trip timings were observed. This is because the "trip on the way in" scheme issues trip signals prior to actual pole slip. Fig. 10 shows the impedance trajectories, blinders and supervisory Mho circle used in the study. In addition, impedance based schemes are inherently slower compared to the instantaneous value based techniques due to use of Discrete Fourier Transform (DFT) based phasor calculation technique. Blinder and timer settings were calculated using critical clearing angle obtained via transient stability simulations and the equations provided in [7].

Fig. 12 shows the estimated relative speed trajectories used by the proposed method to detect an OOS condition. The proposed algorithm detected the OOS condition at the second peak/valley of the unstable ω vs t trajectory at around 0.9s. The instantaneous voltages and currents which were used to estimate relative speed in the proposed algorithm along with the estimated speed are depicted in Fig. 13.

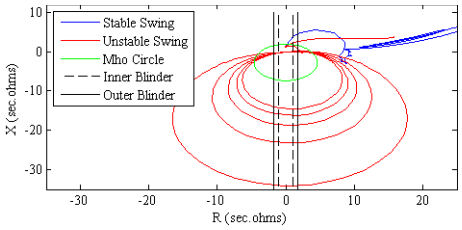

Fig. 10: Impedance trajectories of the double blinder scheme

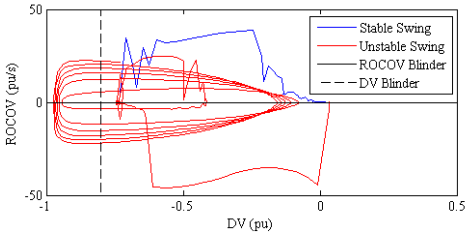

Fig. 11: ROCOV vs DV trajectories of ROCOV OOS scheme

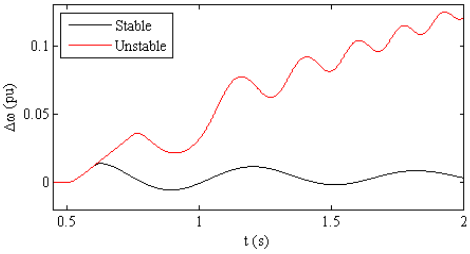

Fig. 12: ω vs t trajectories used by the proposed method

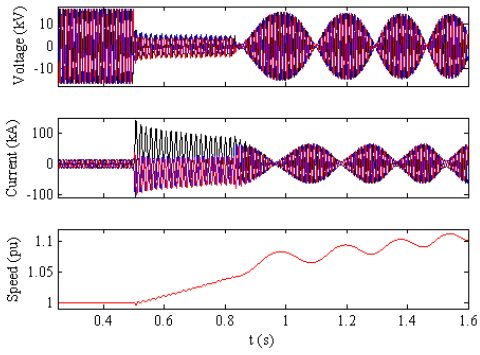

Fig. 13: Generator terminal voltage, current and speed for the unstable power swing scenario

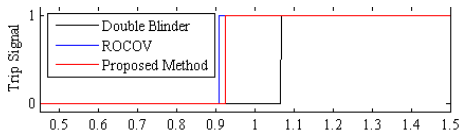

Fig. 14: Trip timings of double blinder, ROCOV and proposed OOS schemes for the unstable power swing

V. Conclusion

This paper proposed a novel method to detect an OOS condition of a generator using its estimated rotor speed. The proposed method monitors the change of rotor speed following a fault and declares the OOS condition if the speed tends to increase or decrease during a swing cycle. The proposed method was implemented as a custom component in an EMT-type program. Several time domain simulation tests were performed and the results were compared against double blinder OOS relay and a rate of change of voltage (ROCOV) based relay. Better or similar OOS detection times were observed and hence the reliability and security of the method is validated. Unlike conventional impedance based algorithms, the threshold settings of the proposed method are not very critical and may not be required to change based on network conditions. This is a significant saving of time and effort for utility engineers. Further verification using field data is required. Application of the proposed method in networks with high penetration of Inverter Based Resources (IBR) will be discussed in a future paper.

References

[1] T. J. Hammons, "Electrical damping and its effect on accumulate fatigue life expenditure of turbine-generator shafts following worst-case supply system disturbances," *IEEE Transactions on Power Apparatus and Systems*, vol. PAS-102, no. 6, pp. 1552–1565, June 1983.

[2] M. McDonald, D. Tziouvaras, A. Apostolov *et al.*, "Power swing and out-of-step considerations on transmission lines," *IEEE PSRC WG D*, vol. 6, p. 2005, 2005.

[3] M. M. Ostojic and M. B. Djuric, "Out-of-step protection of synchronous generators based on a digital phase comparison in the time domain," *IET Generation, Transmission Distribution*, vol. 12, no. 4, pp. 873–879, 2018.

[4] D. Paunescu, F. Lazar, B. Pavlov, and J. Zakonjsek, "Out of step protection in modern power networks," in *2004 8th IEE International Conference on Developments in Power System Protection*, vol. 1, April 2004, pp. 11–14 Vol.1.

[5] J. Berdy, W. A. Elmore, L. E. Goff, W. C. New, G. C. Parr, A. H. Summers, and C. L. Wagner, "Loss of excitation protection for modern synchronous generators," *IEEE Transactions on Power Apparatus and Systems*, vol. 94, no. 5, pp. 1457–1463, Sep. 1975.

[6] M. Rasoulpour, T. Amraee, and A. K. Sedigh, "A relay logic for total and partial loss of excitation protection in synchronous generators," *IEEE Transactions on Power Delivery*, vol. 35, no. 3, pp. 1432–1442, 2020.

[7] IEEE Power System Relaying Committee and others, "Ieee tutorial on the protection of synchronous generators," *IEEE PSRC WG J*, 2011.

[8] Q. Verzosa, "Realistic testing of power swing blocking and out-of-step tripping functions," in *2013 66th Annual Conference for Protective Relay Engineers*, 2013, pp. 420–449.

[9] D. A. Tziouvaras and D. Hou, "Out-of-step protection fundamentals and advancements," in *57th Annual Conference for Protective Relay Engineers, 2004.* IEEE, 2004, pp. 282–307.

[10] M. Aghazadeh and A. Kazemi, "A novel fast algorithm for detecting out-of-step using equal area criterion," in *2016 24th Iranian Conference on Electrical Engineering (ICEE)*, May 2016, pp. 931–936.

[11] E. Farantatos, R. Huang, G. J. Cokkinides, and A. P. Meliopoulos, "A predictive generator out-of-step protection and transient stability monitoring scheme enabled by a distributed dynamic state estimator," *IEEE Transactions on Power Delivery*, vol. 31, no. 4, pp. 1826–1835, Aug 2016.

[12] J. Blumschein, Y. Yelgin, and M. Kereit, "Proper detection and treatment of power swing to reduce the risk of blackouts," in *2008 Third International Conference on Electric Utility Deregulation and Restructuring and Power Technologies*, April 2008, pp. 2440–2446.

[13] J. R. Camarillo-Penaranda, D. Celeita, M. Gutierrez, M. Toro, and G. Ramos, "An approach for out-of-step protection based on swing center voltage estimation and analytic geometry parameters," *IEEE Transactions on Industry Applications*, vol. 56, no. 3, pp. 2402–2408, 2020.

[14] C. W. Taylor, J. M. Haner, L. A. Hill, W. A. Mittelstadt, and R. L. Cresap, "A new out-of-step relay with rate of change of apparent resistance augmentation," *IEEE Power Engineering Review*, vol. PER-3, no. 3, pp. 32–32, 1983.

[15] J. M. Haner, T. D. Laughlin, and C. W. Taylor, "Experience with the r-rdot out-of-step relay," *IEEE Transactions on Power Delivery*, vol. 1, no. 2, pp. 35–39, 1986.

[16] A. Sauhats, A. Utans, and E. Biela-Dalidovicha, "Equal area criterion and angle control-based out-of-step protection," in *2017 IEEE 58th International Scientific Conference on Power and Electrical Engineering of Riga Technical University (RTUCON)*, 2017, pp. 1–6.

[17] M. N. Pala, A. Thakar, and A. Patel, "Power swing and out of step protection using equal area criteria," in *2019 IEEE 5th International Conference for Convergence in Technology (I2CT)*, 2019, pp. 1–7.

[18] V. Centeno, A. G. Phadke, A. Edris, J. Benton, M. Gaudi, and G. Michel, "An adaptive out-of-step relay [for power system protection]," *IEEE Transactions on Power Delivery*, vol. 12, no. 1, pp. 61–71, 1997.

[19] M. A. Redfern and M. J. Checkfield, "A new pole slipping protection algorithm for dispersed storage and generation using the equal area criterion," *IEEE Transactions on Power Delivery*, vol. 10, no. 1, pp. 194–202, 1995.

[20] M. A. Redfern and M. J. Checksfield, "A study into a new solution for the problems experienced with pole slipping protection [of synchronous generators]," *IEEE Transactions on Power Delivery*, vol. 13, no. 2, pp. 394–404, 1998.

[21] S. Paudyal, G. Ramakrishna, and M. S. Sachdev, "Application of equal area criterion conditions in the time domain for out-of-step protection," *IEEE Transactions on Power Delivery*, vol. 25, no. 2, pp. 600–609, 2010.

[22] Shengli Cheng and M. S. Sachdev, "Out-of-step protection using the equal area criterion," in *Canadian Conference on Electrical and Computer Engineering, 2005.*, 2005, pp. 1488–1491.

[23] M. Abedini, M. Davarpanah, M. Sanaye-Pasand, S. M. Hashemi, and R. Iravani, "Generator out-of-step prediction based on faster-than-real-time analysis: Concepts and applications," *IEEE Transactions on Power Systems*, vol. 33, no. 4, pp. 4563–4573, 2018.

[24] K. H. So, J. Y. Heo, C. H. Kim, R. K. Aggarwal, and K. B. Song, "Out-of-step detection algorithm using frequency deviation of voltage," *IET Generation, Transmission Distribution*, vol. 1, no. 1, pp. 119–126, 2007.

[25] B. Shrestha, P. Sharma, and R. Gokaraju, "Out-of-step protection using the analysis of electrical power vs speed deviation in state plane," in *IEEE PES ISGT Europe 2013*, 2013, pp. 1–5.

[26] B. Shrestha, R. Gokaraju, and M. Sachdev, "Out-of-step protection using state-plane trajectories analysis," *IEEE Transactions on Power Delivery*, vol. 28, no. 2, pp. 1083–1093, April 2013.

[27] H. Yaghobi, "Out-of-step protection of generator using analysis of angular velocity and acceleration data measured from magnetic flux," *Electric Power Systems Research*, vol. 132, pp. 9 – 21, 2016.

[28] S. M. Brahma, "Distance relay with out-of-step blocking function using wavelet transform," *IEEE Transactions on Power Delivery*, vol. 22, no. 3, pp. 1360–1366, 2007.

[29] Manitoba HVDC Research Centre, *User's guide on the use of PSCAD*, 5th ed., Manitoba HVDC Research Centre, a division of Manitoba Hydro International Ltd, 211 Commerce Drive, Winnipeg, Manitoba, Canada R3P 1A3, February 2010.

[30] P. Kundur, N. J. Balu, and M. G. Lauby, *Power system stability and control*. McGraw-hill New York, 1994, vol. 7.

[31] S. Filizadeh, *Electric machines and drives: principles, control, modeling, and simulation*. CRC Press, 2013.

[32] R. H. Park, "Two-reaction theory of synchronous machines generalized method of analysis-part i," *Transactions of the American Institute of Electrical Engineers*, vol. 48, no. 3, pp. 716–727, 1929.

[33] D. R. Gurusinghe and A. D. Rajapakse, "Post-disturbance transient stability status prediction using synchrophasor measurements," *IEEE Transactions on Power Systems*, vol. 31, no. 5, pp. 3656–3664, 2016.

[34] J. J. Grainger and W. D. Stevenson, *Power system analysis*. McGraw-Hill New York, 1994, vol. 67.